UNIVERSITAT POLITÈCNICA DE CATALUNYA BARCELONATECH

IEEC

White dwarf collisions: a new pathway to type Ia supernovae

Enrique García-Berro & Pablo Lorén-Aguilar

Supernovae, hypernovae and binary driven hypernovae

An Adriatic Workshop – Pescara 2016

CONTENTS

CONTENTS

CONTENTS
1. Introduction

1. INTRODUCTION
1.1 White dwarf interactions

- A large fraction of stars belong to binary systems or, more generally, to multiple systems.
- A substantial number of these binary systems are so close that at a given time of their life a mass transfer episode will occur.
- Moreover, in dense stellar systems single stars pass very close each other.
- The study of the interactions between two white dwarfs has received considerable interest in the last 30 years, since it has been shown that, in some cases, the result of such interactions is a Type Ia supernova outburst.

1. INTRODUCTION
1.1 White dwarf interactions

- The effort of producing Type Ia supernovae in white dwarf dynamical interactions has been only partially successful, and only under certain circumstances a powerful detonation ensues.

1. INTRODUCTION
1.1 White dwarf interactions

- Even if dynamical interactions fail in producing a supernova outburst, they can still be responsible of some other interesting phenomena:
  - R Corona Borealis stars
  - High-field magnetic white dwarfs
  - Anomalous X-Ray pulsars
  - Pollute the ISM
  - Powerful sources of gravitational waves
- Thus, for multiple reasons the interactions of two white dwarfs is a subject that deserves to be studied in detail.

1. INTRODUCTION
1.2 Type Ia supernovae scenarios

- There are several possible scenarios:
  - Single degenerate (SD): WD + RG star (Whelan & Iben 1973)
  - Double degenerate (DD): WD + WD in a binary system (Webbink 1984; Iben & Tutukov 1984)
  - Core degenerate (CD): WD + core of an AGB star (Livio & Riess 2003)
  - Collisions (WDC): WD + WD in dense stellar systems (Raskin et al. 2009)
- I will review two of them: the WDC and the CD scenarios.

CONTENTS

CONTENTS
1. Introduction

2. White dwarf collisions
2.1 Motivation

- Globular clusters are stellar systems made of 10^4-10^7 stars, have high core densities of around 10^3 pc^{-3}, are old (have ages around 10-13 Gyr), and thus contain many degenerate objects.
- Also, the central regions of galaxies have very high stellar densities. In such a dense environment stars can pass very close one to another.
- During the lifetime of the cluster every star will suffer one or more of these events, leading to the formation of binaries, through gravitational focusing or to the emission of gravitational waves, and to collisions.

2. White dwarf collisions
2.1 Motivation

- It has been predicted that the white dwarf merger rate leading to super-Chandrasekhar remnants will be increased by an order of magnitude through dynamical interactions (Shara & Hurley 2002).
- Also, dynamical interactions in globular clusters and in the central regions of galaxies can form double white dwarfs with non-zero eccentricities, which will be detectable by LISA (Willems et al. 2007).

2. White dwarf collisions
2.2 Studies of white dwarf collisions

- The study of white dwarf collisions was pioneered by Benz et al. (1989), who employed a SPH code to simulate the collisions of two systems of white dwarfs of masses 0.6 $M_\odot$ and 0.6 $M_\odot$, and 0.9 $M_\odot$ and 0.7$_\odot$ M.
- The first recent study of white dwarf collisions was performed by Rosswog et al. (2009), but limited to head-on collisions.
- Almost simultaneously, Raskin et al. (2009) examined the collision of two otherwise typical white dwarfs of equal masses (0.6 $M_\odot$).

2. White dwarf collisions
2.2 Studies of white dwarf collisions

- Lorén-Aguilar et al. (2010) explored the collisions of one mass pair (of unequal masses, 0.6 $M_\odot$ and 0.8 $M_\odot$) for various impact parameters.
- Raskin et al. (2010) expanded their previous study to encompass pairs of dierent masses and collisions with dierent impact parameters.
- García-Senz et al. (2013) studied the head-on collision of two twin white dwarfs of mass 0.7 $M_\odot$, but although they used a very high mass resolution, the simulations were not three-dimensional.

2. White dwarf collisions
2.2 Studies of white dwarf collisions

- The only studies in which a SPH code was not employed are those of Hawley et al. (2012) and Papish & Perets (2016). In both cases the Eulerian adaptive grid code FLASH was used.
- Hawley et al. (2012) studied two twin pairs of masses 0.64 $M_\odot$, and 0.81 $M_\odot$.
- Papish & Perets (2016) considered several masses of the colliding white dwarfs, from 0.6 $M_\odot$ to 0.8 $M_\odot$.
- Aznar-Siguán et al. (2013) computed a grid of white dwarf collisions, considering a large interval of initial conditions and a broad range of masses and chemical compositions of the interacting objects.

2. White dwarf collisions
2.2 Studies of white dwarf collisions

- This suite of calculations together with that of Raskin et al. (2010) are the most comprehensive set of calculations of white dwarf collisions performed so far.
- The advantage of the simulations of Aznar-Siguán et al. (2013) over the rest of theoretical calculations is that they explored the role of the composition of the colliding white dwarfs.
- They computed collisions in which one of the components of the pair of white dwarfs was made of He, or ONe, while the second white dwarf was made of CO or He.

CONTENTS

CONTENTS
3.Smoothed Particle Hydrodynamics

3. Smoothed Particle Hydrodynamics
3.1 SPH generalities

- SPH is an approximate method to solve the fluid dynamics equations.
- The fluid elements are replaced by particles of finite size.
- Fully Lagrangian method.
- Mathematicians would think about these particles as interpolation points on a moving grid.
- Physicist think about them as regular particles, moving under the action of normal forces.

3. Smoothed Particle Hydrodynamics
3.1 SPH generalities

- It is used a kernel estimation technique to estimate probability densities from sample values.
- Can be used to interpolate anywhere at any time.
- Interesting features:

  - Advection is treated in a very natural way. Hence, transport phenomena occur naturally.
  - We do not have a fixed grid.
  - Resolution is dependent on both space and time, without rezoning.
  - Complex physics can be easily introduced.

3. Smoothed Particle Hydrodynamics
3.1 SPH generalities

- The SPH algorithm gives very satisfactory results for shocks though they are not as accurate as those obtained from well-designed Riemann solvers and other modern techniques.

3. Smoothed Particle Hydrodynamics
3.2 Numerical setup

- Cubic spline (Monaghan & Lattanzio 1985).
- Octree (Barnes & Hut 1986).
- Smoothing lengths: iteration method (Price & Monaghan 2007).
- Artificial viscosity based on Riemann solvers (Monaghan 1997), variable viscosity parameters of Morris & Monaghan (1997) and switch of Balsara (1995).
- Predictor-corrector numerical scheme with variable timestep (Serna et al., 1996).
- Time steps are the same for all particles.
- Message Passage Interface (MPI) libraries.

3. Smoothed Particle Hydrodynamics
3.3 Physical inputs

- Simultaneous evolution of the energy and temperature.
- Helmholtz EOS (Timmes & Swesty 2000).
- Nuclear network:
  - 14 nuclei: He, C, O, Ne, Mg, Si, S, Ar, Ca, Ti, Cr, Fe, Ni, Zn.
  - Reactions: captures of α particles, associated back reactions, fusion of two C nuclei, reactions between C and O and between two O nuclei.
  - REACLIB database (Cyburt et al. 2010).
- Neutrino emissivity (Itoh et al. 1997).

3. Smoothed Particle Hydrodynamics
3.4 Other features

- Gravitational wave radiation is computed in the slow-motion, weak-field quadrupole approximation, transverse-traceless gauge:

$$h_{ij}^{TT}(t,x) = \frac{2G}{c^4 d}\frac{\partial^2 Q_{jk}^{TT}(t-R)}{\partial t^2}$$

$$h_{ij}{}^{TT}(t) \approx P_{ijkl}(N)\sum_{p=1}^{n} m(p)[2v^k(p)v^l(p) + x^k(p)a^l(p) + a^k(p)x^l(p)]$$

CONTENTS

CONTENTS
4.Some results

4. SOME RESULTS
4.1 Initial conditions

- We consider five white dwarfs with masses 0.4, 0.6, 0.8 and 1.0 $M_{\odot}$, with the appropriate composition (He, CO and ONe), plus one additional calculation.
- The initial trajectories are elliptical, corresponding to a post-capture scenario.

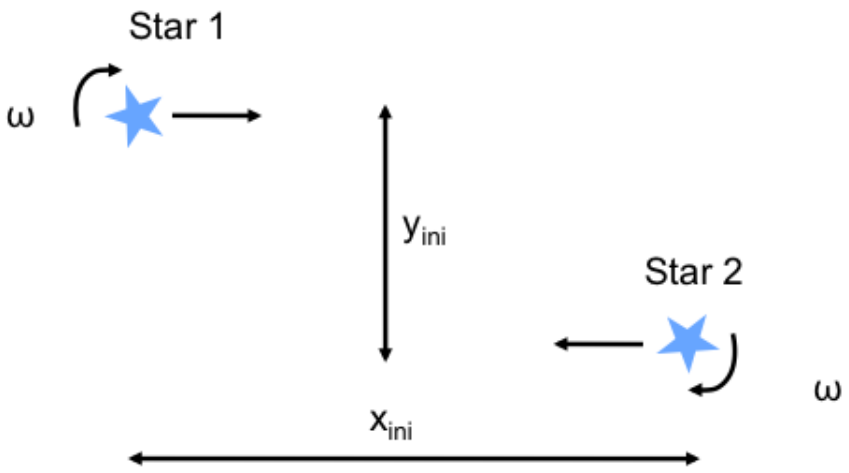

4. SOME RESULTS
4.1 Initial conditions: 0.6 $M_\odot$ + 0.8 $M_\odot$

Run	y_{ini} ($R_\odot$)	v_{ini} (km/s)	Outcome	E (10^{48} erg)	L (10^{50} erg/s)	r_{max} (0.1 $R_\odot$)	r_{min} (0.1 $R_\odot$)	ε	β
1	0.8	100	O	−2.13	7.49	8.28	0.50	0.886	0.40
2	0.5	150	O	−3.17	7.02	5.46	0.45	0.848	0.44
3	0.5	50	DC	−3.44	2.33	5.39	0.05	0.983	4.00
4	0.3	225	O	−4.49	6.31	3.80	0.37	0.823	0.54
5	0.3	200	LC	−4.64	5.62	3.75	0.29	0.858	0.69
6	0.3	175	LC	−4.77	4.91	3.71	0.21	0.891	0.95
7	0.3	150	LC	−4.88	4.21	3.68	0.16	0.919	1.25
8	0.3	125	LC	−4.98	3.51	3.66	0.11	0.943	1.82
9	0.3	100	DC	−5.05	2.81	3.64	0.07	0.964	2.86
10	0.1	200	DC	−7.82	1.87	2.36	0.03	0.975	6.67
11	0.1	150	DC	−8.06	1.40	2.31	0.02	0.986	10.0
12	0.1	120	DC	−8.16	1.17	2.28	0.01	0.990	20.0

$$b = \frac{R_1 + R_2}{r_{min}}$$

4. SOME RESULTS
4.1 Initial conditions: full set.

Table 1. Kinematical properties of the simulations reported here involving a $0.8\,M_\odot$ white dwarf.

Run	M_1+M_2 $(M_\odot)$	Outcome	Detonation	E $(10^{48}$ erg$)$	L $(10^{50}$ erg s$^{-1})$	r_{max} $(R_\odot)$	r_{min} $(R_\odot)$	ϵ	β
$v_{ini}=75$ km/s	$\Delta y=0.4\,R_\odot$								
1	0.8+0.6	DC	Y	−4.12	2.80	4.48×10^{-1}	6.72×10^{-3}	0.970	2.83
2	0.8+0.8	DC	Y	−5.49	3.28	4.49×10^{-1}	5.88×10^{-3}	0.974	3.06
3	1.0+0.8	DC	B	−6.88	3.64	4.49×10^{-1}	5.21×10^{-3}	0.977	3.07
4	1.2+0.8	DC	L	−8.26	3.93	4.48×10^{-1}	4.70×10^{-3}	0.980	2.98
$v_{ini}=100$ km/s	$\Delta y=0.5\,R_\odot$								
5	0.8+0.6	DC	Y	−5.05	2.81	3.64×10^{-1}	6.76×10^{-3}	0.964	2.81
6	0.8+0.8	DC	Y	−6.76	3.28	3.63×10^{-1}	5.90×10^{-3}	0.968	3.05
7	1.0+0.8	DC	B	−8.47	3.64	3.63×10^{-1}	5.25×10^{-3}	0.972	3.06
8	1.2+0.8	DC	L	−10.1	3.93	3.63×10^{-1}	4.71×10^{-3}	0.974	2.97
$v_{ini}=100$ km/s	$\Delta y=0.4\,R_\odot$								
9	0.8+0.6	LC	Y	−4.06	3.74	4.49×10^{-1}	1.21×10^{-2}	0.948	1.57
10	0.8+0.8	LC	Y	−5.42	4.37	4.50×10^{-1}	1.06×10^{-2}	0.954	1.71
11	1.0+0.8	LC	Y	−6.80	4.85	4.50×10^{-1}	9.35×10^{-3}	0.959	1.71
12	1.2+0.8	LC	Y	−8.18	5.24	4.49×10^{-1}	8.42×10^{-3}	0.963	1.66
$v_{ini}=150$ km/s	$\Delta y=0.5\,R_\odot$								
13	0.8+0.6	LC	N	−4.88	4.21	3.68×10^{-1}	1.56×10^{-2}	0.919	1.22
14	0.8+0.8	LC	Y	−6.56	4.91	3.67×10^{-1}	1.35×10^{-2}	0.929	1.33
15	1.0+0.8	LC	Y	−8.25	5.46	3.66×10^{-1}	1.20×10^{-2}	0.937	1.33
16	1.2+0.8	LC	Y	−9.93	5.90	3.66×10^{-1}	1.08×10^{-2}	0.943	1.30
$v_{ini}=150$ km/s	$\Delta y=0.4\,R_\odot$								
17	0.8+0.6	LC	N	−3.89	5.60	4.53×10^{-1}	2.81×10^{-2}	0.883	0.68
18	0.8+0.8	LC	N	−5.22	6.55	4.54×10^{-1}	2.45×10^{-2}	0.898	0.73
19	1.0+0.8	LC	N	−6.57	7.28	4.53×10^{-1}	2.16×10^{-2}	0.909	0.74
20	1.2+0.8	LC	Y	−7.93	7.86	4.52×10^{-1}	1.94×10^{-2}	0.918	0.72
$v_{ini}=200$ km/s	$\Delta y=0.5\,R_\odot$								
21	0.8+0.6	LC	N	−4.64	5.62	3.75×10^{-1}	2.86×10^{-2}	0.858	0.66
22	0.8+0.8	LC	N	−6.28	6.55	3.73×10^{-1}	2.48×10^{-2}	0.875	0.73
23	1.0+0.8	LC	N	−7.94	7.28	3.72×10^{-1}	2.18×10^{-2}	0.889	0.73
24	1.2+0.8	LC	Y	−9.61	7.86	3.70×10^{-1}	1.96×10^{-2}	0.900	0.71
$v_{ini}=200$ km/s	$\Delta y=0.4\,R_\odot$								
25	0.8+0.6	O	N	−3.65	7.47	4.61×10^{-1}	5.28×10^{-2}	0.796	0.36
26	0.8+0.8	O	N	−4.94	8.74	4.60×10^{-1}	4.54×10^{-2}	0.820	0.40
27	1.0+0.8	O	N	−6.26	9.70	4.58×10^{-1}	3.99×10^{-2}	0.840	0.40
28	1.2+0.8	O	N	−7.60	10.50	4.57×10^{-1}	3.56×10^{-2}	0.855	0.39
$v_{ini}=300$ km/s	$\Delta y=0.5\,R_\odot$								
29	0.8+0.6	O	N	−5.97	8.39	4.02×10^{-1}	6.96×10^{-2}	0.705	0.27
30	0.8+0.8	O	N	−5.47	9.32	3.96×10^{-1}	6.02×10^{-2}	0.736	0.30
31	1.0+0.8	O	N	−7.04	10.00	3.90×10^{-1}	5.27×10^{-2}	0.762	0.30
32	1.2+0.8	O	N	−8.64	11.80	3.86×10^{-1}	4.69×10^{-2}	0.783	0.30
$v_{ini}=300$ km/s	$\Delta y=0.4\,R_\odot$								
33	0.8+0.6	O	N	−2.94	11.20	5.01×10^{-1}	1.35×10^{-1}	0.576	0.14
34	0.8+0.8	O	N	−4.13	13.10	4.89×10^{-1}	1.15×10^{-1}	0.620	0.16
35	1.0+0.8	O	N	−5.37	14.62	4.82×10^{-1}	9.97×10^{-2}	0.657	0.16
36	1.2+0.8	O	N	−6.63	15.71	4.76×10^{-1}	8.81×10^{-2}	0.688	0.16

Table 2. Kinematical properties of the simulations reported here involving a $0.4\,M_\odot$ white dwarf.

Run	M_1+M_2 $(M_\odot)$	Outcome	Detonation	E $(10^{48}$ erg$)$	L $(10^{50}$ erg s$^{-1})$	r_{max} $(R_\odot)$	r_{min} $(R_\odot)$	ϵ	β
$v_{ini}=75$ km/s	$\Delta y=0.5\,R_\odot$								
37	0.2+0.4	DC	L	−0.84	0.82	3.65×10^{-1}	8.94×10^{-3}	0.952	3.97
38	0.4+0.4	DC	B	−1.69	1.23	3.64×10^{-1}	6.65×10^{-3}	0.964	4.21
$v_{ini}=75$ km/s	$\Delta y=0.4\,R_\odot$								
39	0.2+0.4	LC	N	−0.67	1.09	4.51×10^{-1}	1.60×10^{-2}	0.931	2.21
40	0.4+0.4	DC	B	−1.35	1.64	4.50×10^{-1}	1.19×10^{-2}	0.948	2.35
41	0.8+0.4	DC	L	−2.73	2.18	4.49×10^{-1}	7.85×10^{-3}	0.966	2.93
42	1.2+0.4	DC	L	−4.12	2.46	4.48×10^{-1}	5.84×10^{-3}	0.974	3.26
$v_{ini}=100$ km/s	$\Delta y=0.5\,R_\odot$								
43	0.2+0.4	LC	N	−0.81	1.09	3.68×10^{-1}	1.62×10^{-2}	0.916	2.19
44	0.4+0.4	DC	B	−1.65	1.64	3.66×10^{-1}	1.20×10^{-2}	0.937	2.34
45	0.8+0.4	DC	L	−3.35	2.18	3.64×10^{-1}	7.88×10^{-3}	0.958	2.92
46	1.2+0.4	DC	L	−5.07	2.46	3.63×10^{-1}	5.88×10^{-3}	0.968	3.23
$v_{ini}=100$ km/s	$\Delta y=0.4\,R_\odot$								
47	0.2+0.4	LC	N	−0.64	1.46	4.55×10^{-1}	2.96×10^{-2}	0.879	1.21
48	0.4+0.4	LC	N	−1.31	2.18	4.53×10^{-1}	2.16×10^{-2}	0.909	1.29
49	0.8+0.4	DC	L	−2.68	2.91	4.51×10^{-1}	1.42×10^{-2}	0.939	1.62
50	1.2+0.4	DC	L	−4.07	3.27	4.50×10^{-1}	1.05×10^{-2}	0.954	1.80
$v_{ini}=150$ km/s	$\Delta y=0.5\,R_\odot$								
51	0.2+0.4	LC	N	−0.74	1.64	3.81×10^{-1}	3.84×10^{-2}	0.818	0.92
52	0.4+0.4	LC	N	−1.55	2.46	3.75×10^{-1}	2.81×10^{-2}	0.861	1.00
53	0.8+0.4	DC	L	−3.22	3.27	3.69×10^{-1}	1.83×10^{-2}	0.906	1.26
54	1.2+0.4	DC	L	−4.92	3.68	3.67×10^{-1}	1.35×10^{-2}	0.929	1.41
$v_{ini}=150$ km/s	$\Delta y=0.4\,R_\odot$								
55	0.2+0.4	O	N	−0.58	2.18	4.70×10^{-1}	7.14×10^{-2}	0.736	0.50
56	0.4+0.4	O	N	−1.21	3.28	4.62×10^{-1}	5.16×10^{-2}	0.799	0.54
57	0.8+0.4	LC	N	−2.55	4.37	4.56×10^{-1}	3.30×10^{-2}	0.864	0.70
58	1.2+0.4	LC	N	−3.91	4.91	4.54×10^{-1}	2.44×10^{-2}	0.898	0.78
$v_{ini}=200$ km/s	$\Delta y=0.5\,R_\odot$								
59	0.2+0.4	O	N	−0.65	2.18	4.07×10^{-1}	7.31×10^{-2}	0.695	0.49
60	0.4+0.4	O	N	−1.41	3.28	3.90×10^{-1}	5.27×10^{-2}	0.762	0.53
61	0.8+0.4	LC	N	−3.09	4.95	3.78×10^{-1}	3.36×10^{-2}	0.837	0.68
62	1.2+0.4	LC	N	−4.71	4.91	3.73×10^{-1}	2.47×10^{-2}	0.876	0.77
$v_{ini}=200$ km/s	$\Delta y=0.4\,R_\odot$								
63	0.2+0.4	O	N	−0.48	2.91	5.05×10^{-1}	1.41×10^{-1}	0.564	0.25
64	0.4+0.4	O	N	−1.07	4.37	4.82×10^{-1}	9.97×10^{-2}	0.657	0.28
65	0.8+0.4	O	N	−2.36	5.82	4.66×10^{-1}	6.23×10^{-2}	0.764	0.37
66	1.2+0.4	LC	N	−3.70	6.55	4.60×10^{-1}	4.58×10^{-2}	0.821	0.42
$v_{ini}=300$ km/s	$\Delta y=0.5\,R_\odot$								
67	0.4+0.4	O	N	−1.01	4.91	4.87×10^{-1}	1.35×10^{-1}	0.571	0.14
68	0.8+0.4	O	N	−2.50	6.55	4.17×10^{-1}	8.35×10^{-2}	0.696	0.28
69	1.2+0.4	O	N	−4.11	7.56	3.96×10^{-1}	6.01×10^{-2}	0.737	0.32
$v_{ini}=300$ km/s	$\Delta y=0.4\,R_\odot$								
70	0.8+0.4	O	N	−1.82	8.74	5.22×10^{-1}	1.63×10^{-1}	0.525	0.14
71	1.2+0.4	O	N	−3.10	9.82	4.90×10^{-1}	1.14×10^{-1}	0.621	0.17

4. SOME RESULTS
4.2 Outcomes

Eccentric orbit, 0.8 $M_\odot$ + 1.0 $M_\odot$

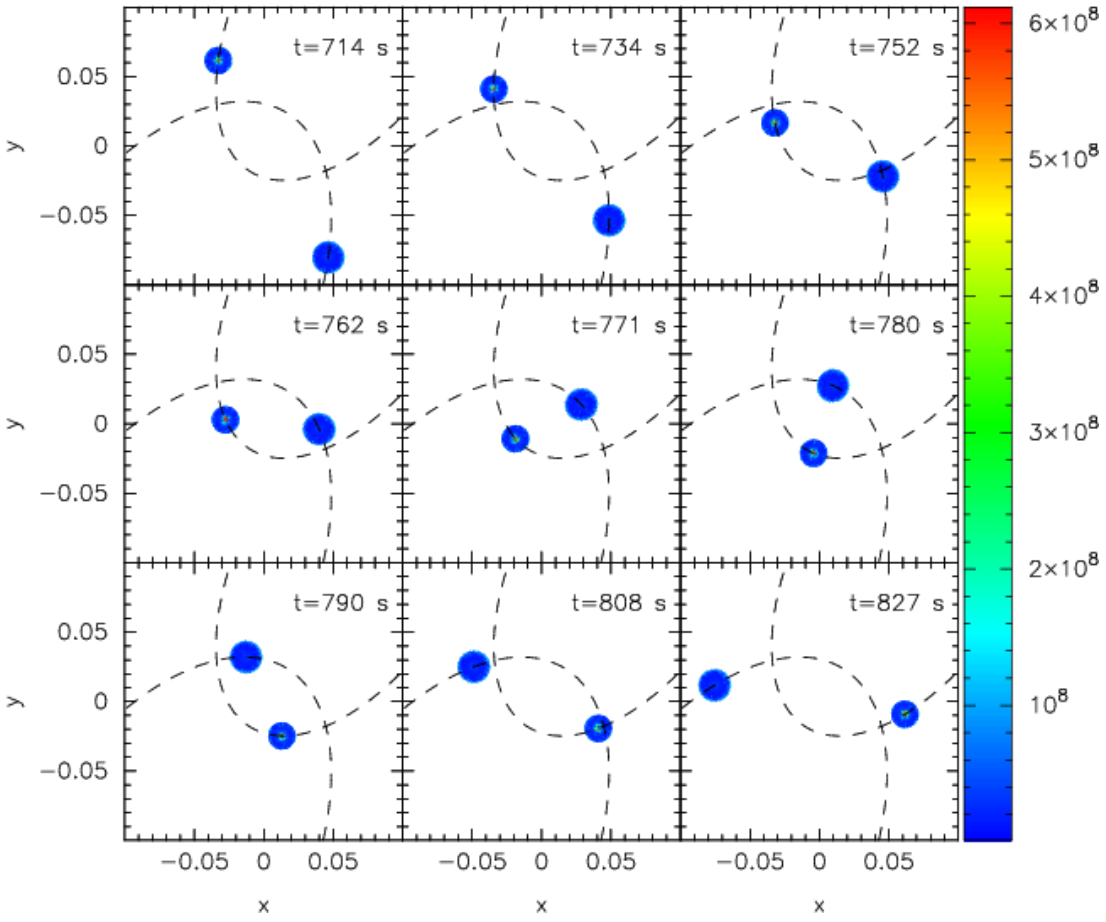

4. SOME RESULTS
4.2 Outcomes

Lateral collision: single remnant

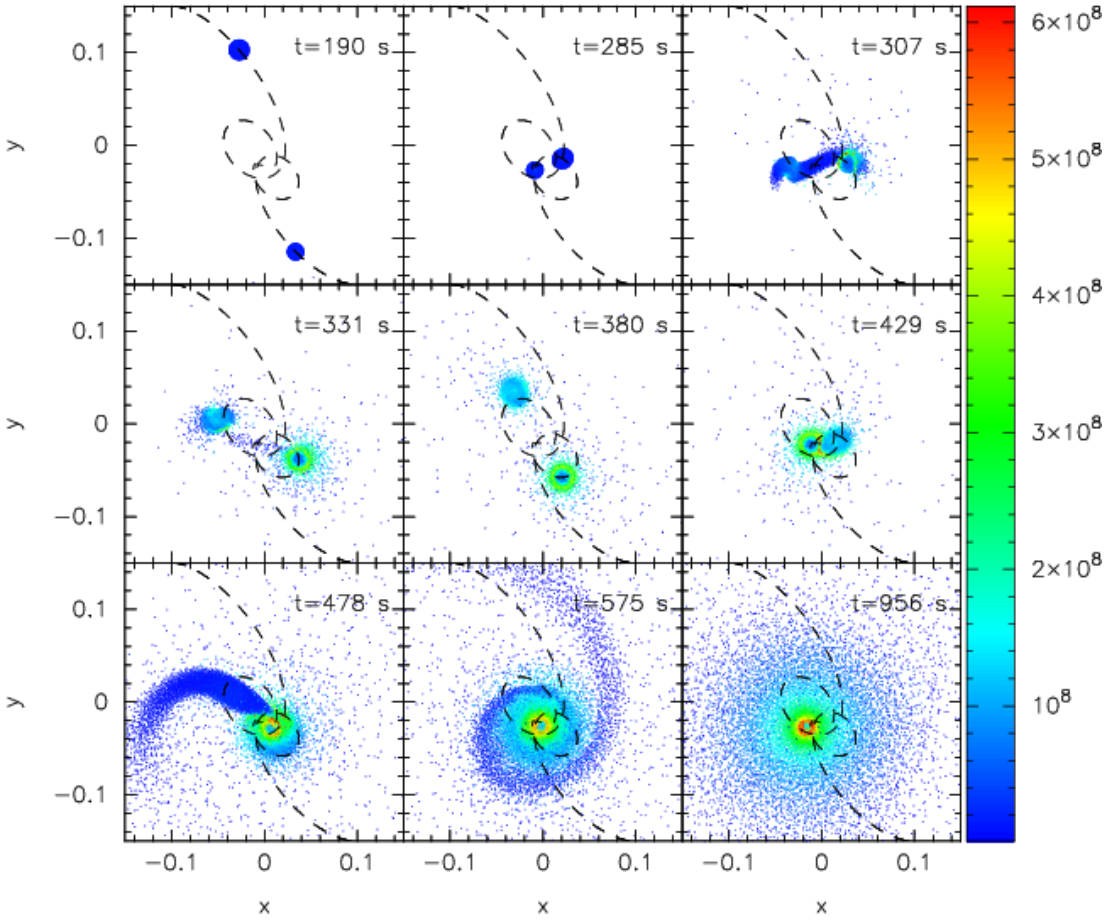

4. SOME RESULTS
4.2 Outcomes

Direct collision: disruption of one star

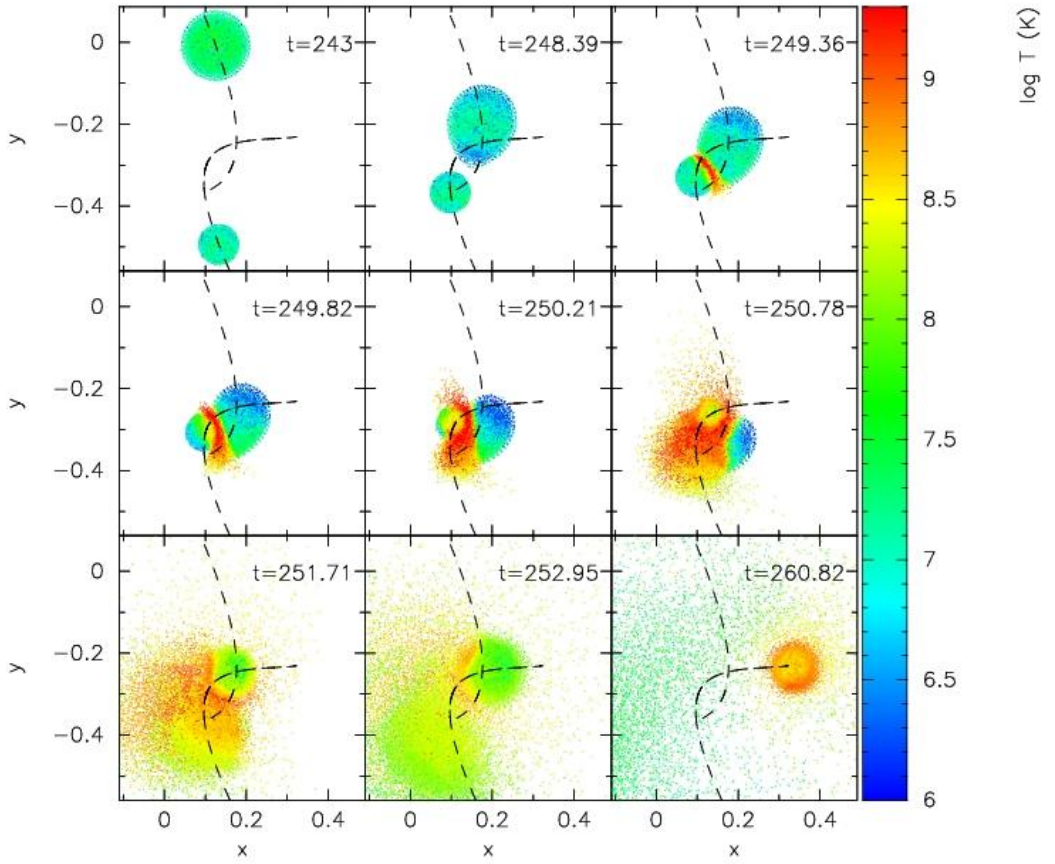

4. SOME RESULTS
4.2 Outcomes

Direct collision: disruption of both stars

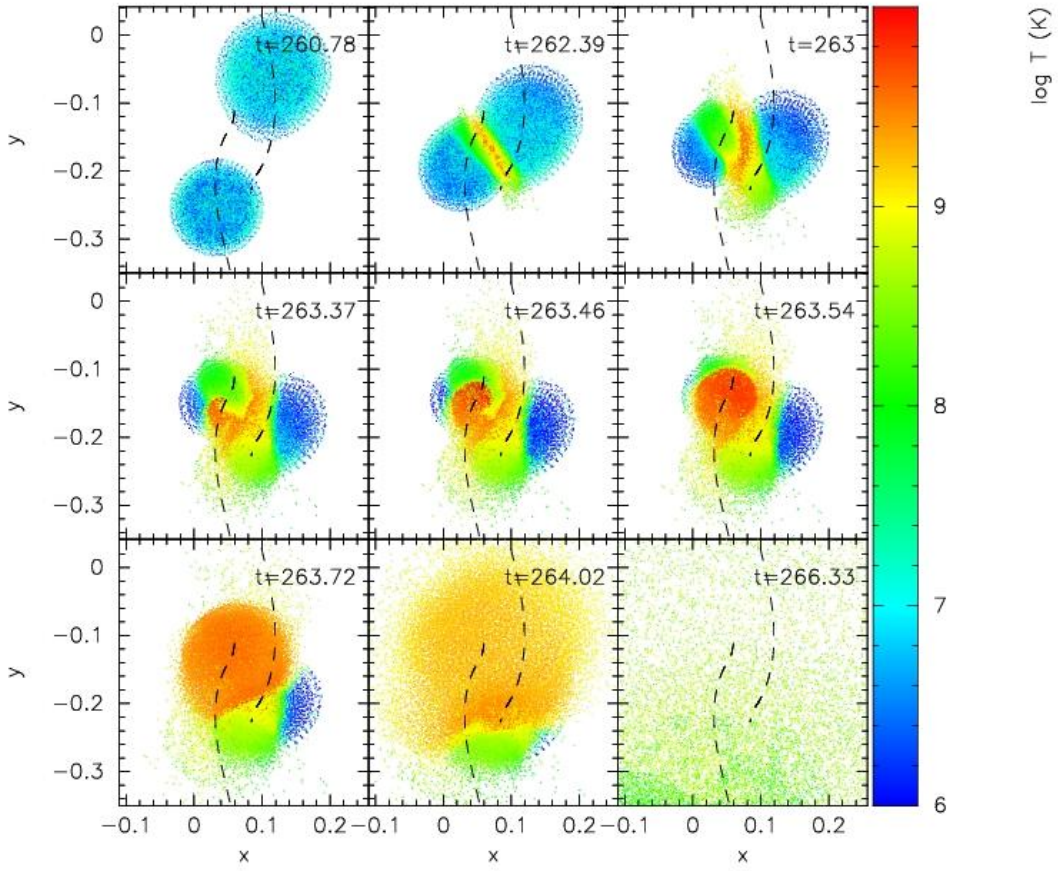

4. SOME RESULTS
4.2 Outcomes

Direct collision: disruption of one star

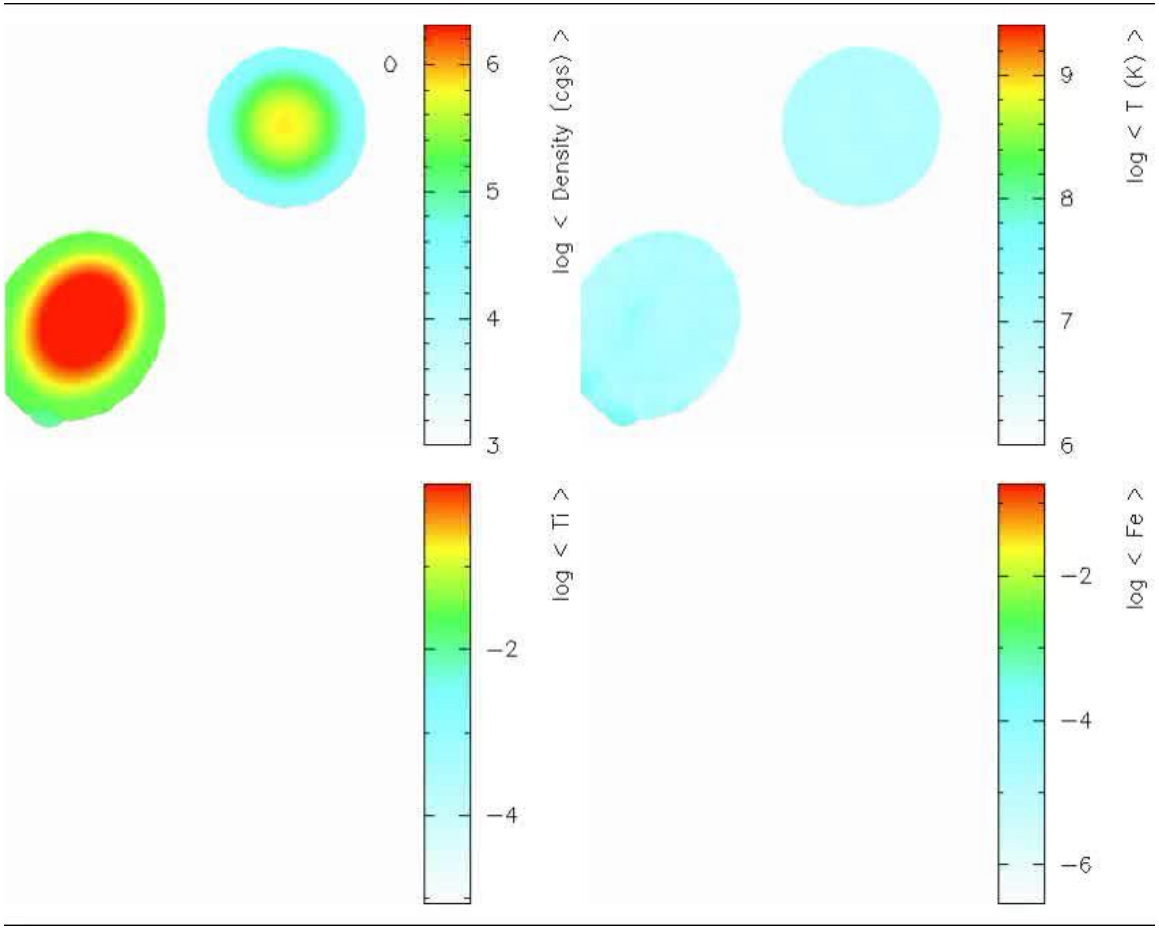

4. SOME RESULTS
4.2 Outcomes

Direct collision: disruption of both stars

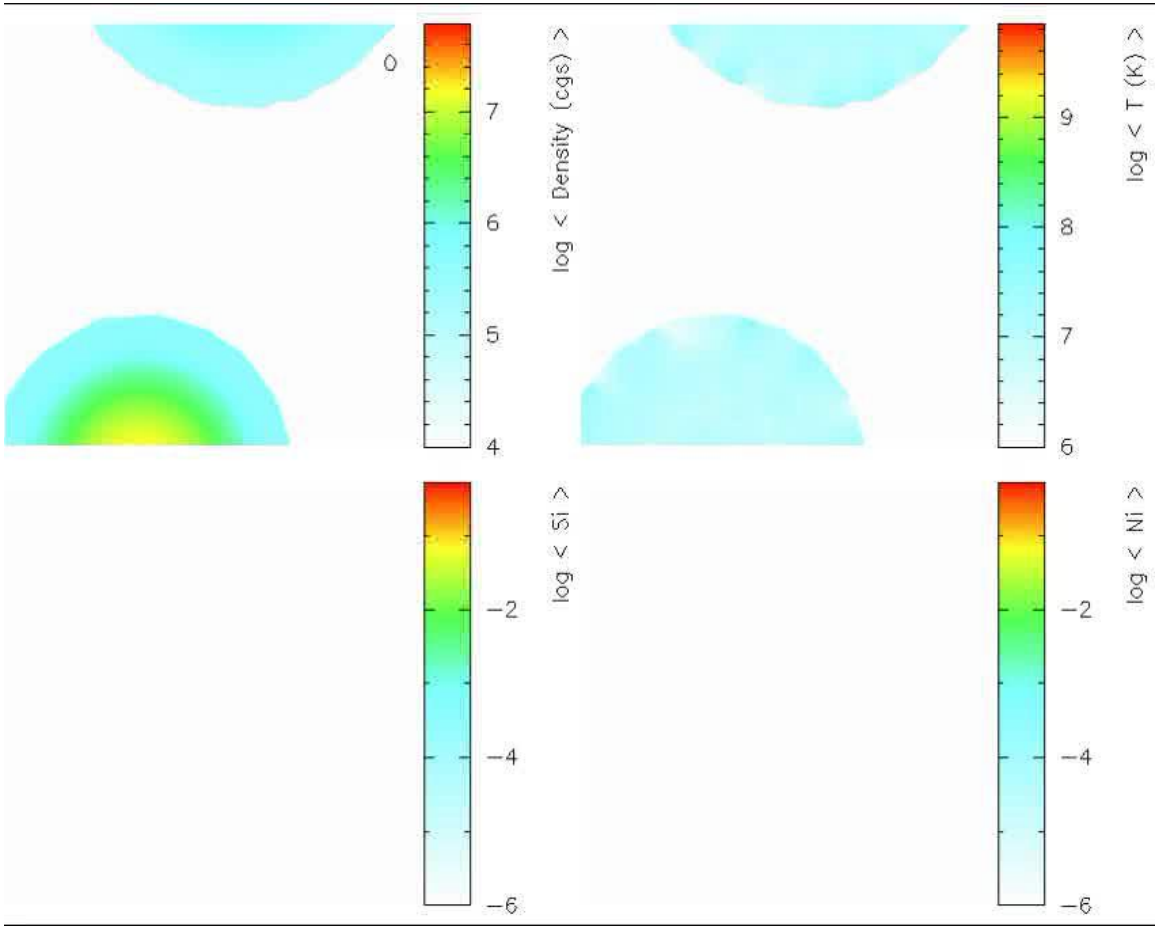

4. SOME RESULTS
4.2 Outcomes

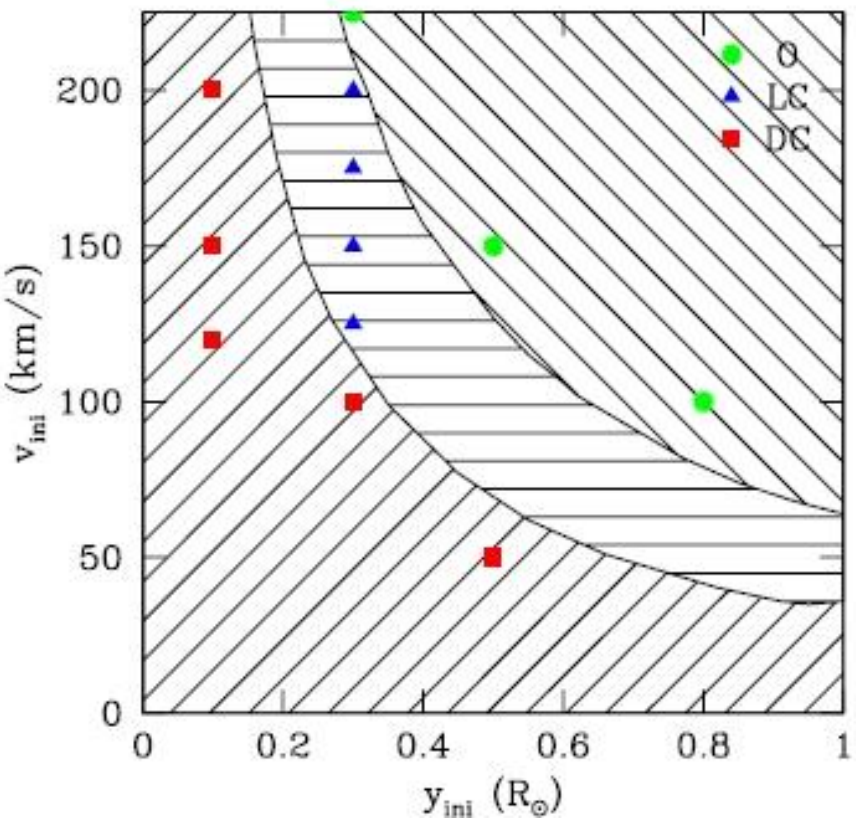

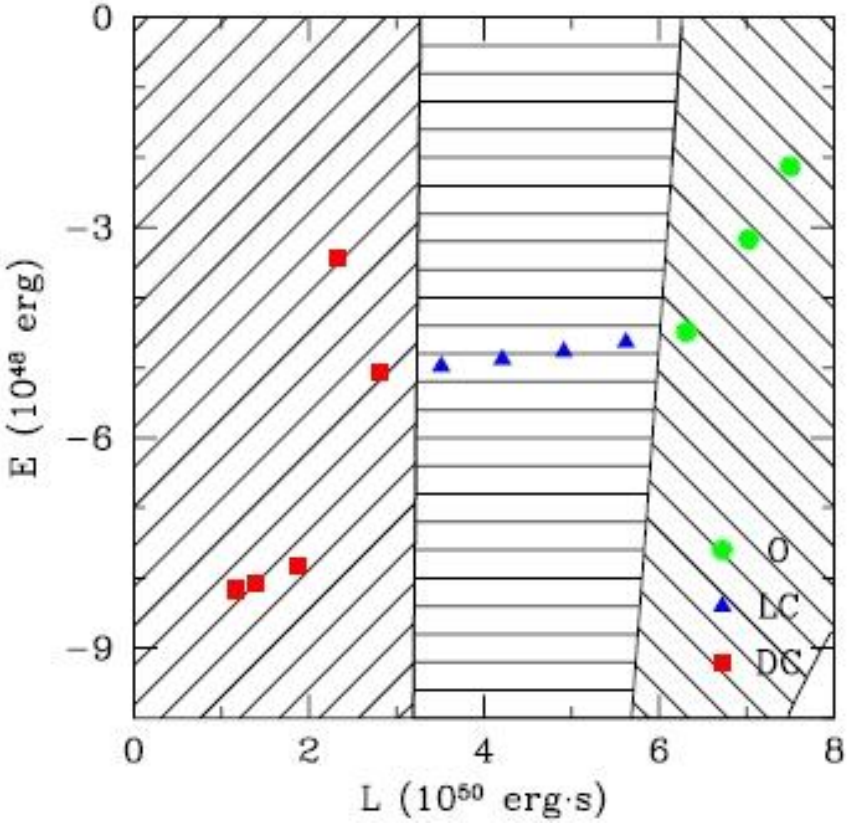

4. SOME RESULTS
4.2 Outcomes

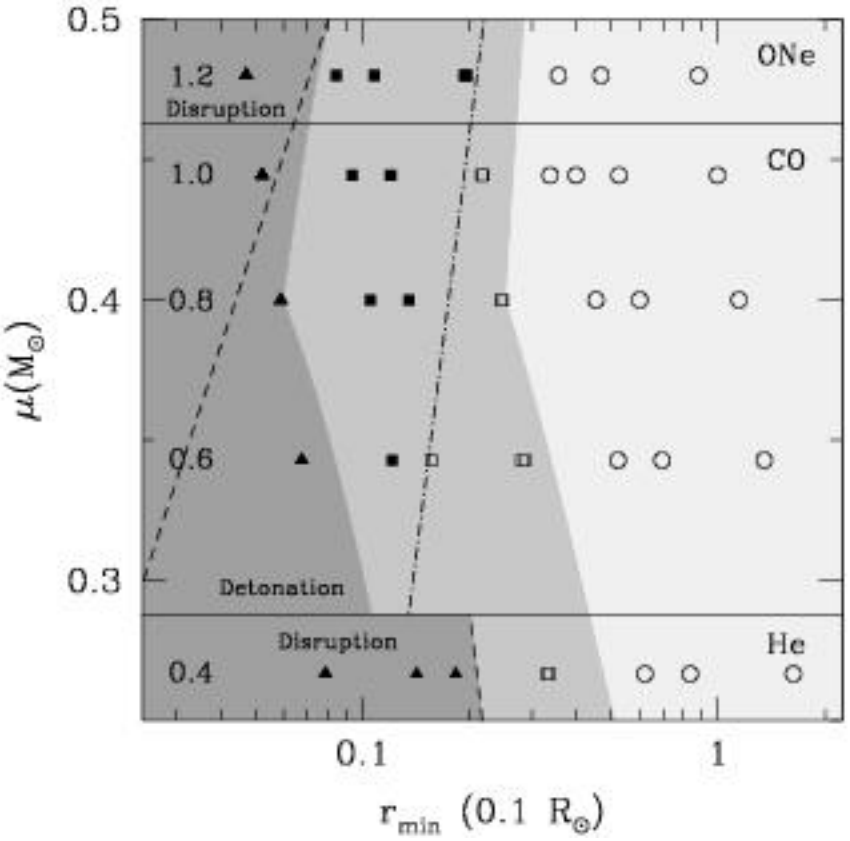

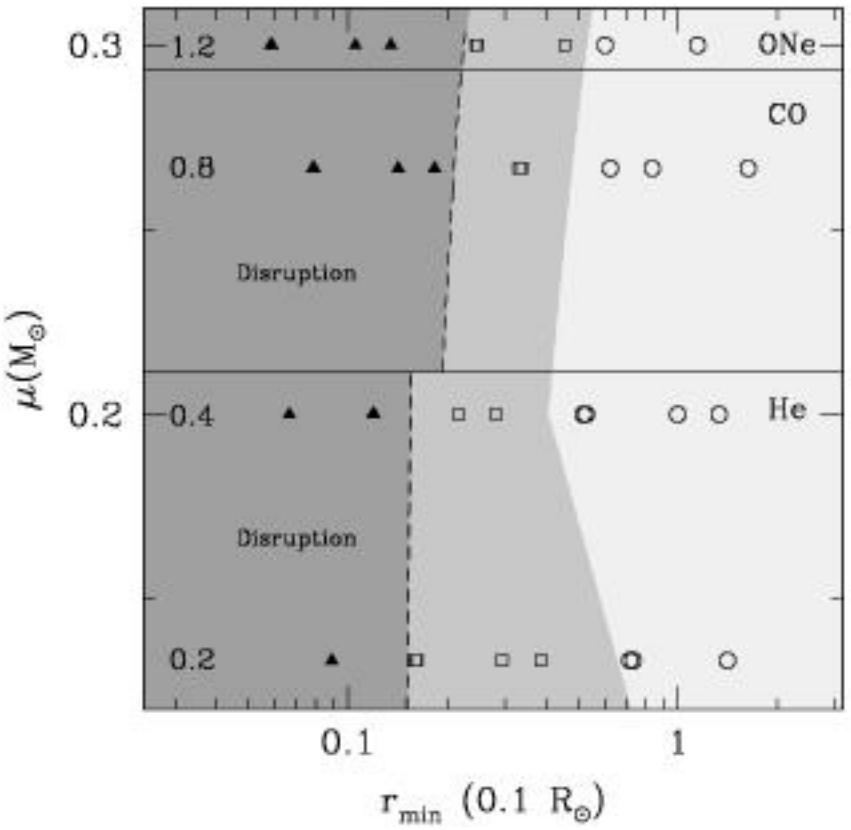

$$r_{\min} = hR_L \approx 0.95R_L$$

$$r_{\min} = lR_1 + R_2 = -0.35R_1 + R_2$$

4. SOME RESULTS
4.3 Characteristics of the interactions

Table 3. Hydrodynamical results for the simulations in which a collision occurs and the resulting system remains bound.

Run	Detonation ($M_\odot$)	M_{WD}	M_{corona} ($M_\odot$)	M_{debris} ($M_\odot$)	M_{ej} ($M_\odot$)	T_{max} (K)	T_{peak} (K)	R_{corona} ($R_\odot$)	R_{debris} ($R_\odot$)	E_{nuc} (erg)
1	Yes	0.90	0.79	0.46	3.74×10^{-2}	5.35×10^{8}	4.37×10^{9}	9.64×10^{-3}	0.43	1.09×10^{49}
2	Yes	1.12	—	0.34	1.41×10^{-1}	4.69×10^{8}	5.44×10^{9}	—	0.28	4.57×10^{49}
5	Yes	0.87	0.79	0.50	3.22×10^{-2}	4.90×10^{8}	4.50×10^{9}	8.86×10^{-3}	0.22	9.81×10^{48}
6	Yes	1.13	—	0.33	1.37×10^{-1}	4.65×10^{8}	5.37×10^{9}	—	0.19	4.25×10^{49}
9	Yes	0.91	0.72	0.48	1.39×10^{-2}	4.79×10^{8}	3.03×10^{9}	8.00×10^{-3}	0.21	9.93×10^{47}
10	Yes	1.29	—	0.28	2.63×10^{-2}	4.50×10^{8}	4.20×10^{9}	—	0.21	2.27×10^{48}
11	Yes	1.12	0.89	0.64	4.64×10^{-2}	7.77×10^{8}	4.51×10^{9}	6.93×10^{-3}	0.24	1.66×10^{49}
12	Yes	1.26	0.54	0.64	1.01×10^{-1}	1.08×10^{9}	4.66×10^{9}	4.98×10^{-3}	0.21	3.67×10^{49}
13	No	0.91	0.71	0.48	7.96×10^{-3}	4.49×10^{8}	2.18×10^{9}	8.05×10^{-3}	0.22	1.49×10^{46}
14	Yes	1.30	—	0.29	8.44×10^{-3}	4.44×10^{8}	3.50×10^{9}	—	0.23	5.24×10^{47}
15	Yes	1.15	0.83	0.63	1.85×10^{-2}	7.54×10^{8}	3.89×10^{9}	6.62×10^{-3}	0.20	2.63×10^{48}
16	Yes	1.26	0.54	0.67	6.81×10^{-2}	1.07×10^{9}	4.30×10^{9}	5.02×10^{-3}	0.19	2.36×10^{49}
17	No	0.91	0.41	0.47	1.41×10^{-2}	4.36×10^{8}	1.16×10^{9}	5.44×10^{-3}	0.38	1.88×10^{41}
18	No	1.38	—	0.21	5.76×10^{-3}	3.49×10^{8}	2.54×10^{9}	—	0.25	7.95×10^{46}
19	No	1.16	0.63	0.62	1.71×10^{-2}	7.02×10^{8}	2.08×10^{9}	4.85×10^{-3}	0.37	8.17×10^{45}
20	Yes	1.31	0.44	0.66	2.70×10^{-2}	1.25×10^{9}	2.80×10^{9}	3.65×10^{-3}	0.36	1.43×10^{48}
21	No	0.92	0.42	0.46	1.39×10^{-2}	4.21×10^{8}	9.22×10^{8}	5.43×10^{-3}	0.49	1.90×10^{39}
22	No	1.33	—	0.27	4.80×10^{-3}	2.48×10^{8}	1.32×10^{9}	—	0.43	8.67×10^{43}
23	No	1.17	0.50	0.62	1.73×10^{-2}	7.56×10^{8}	1.79×10^{9}	4.81×10^{-3}	0.34	9.95×10^{45}
24	Yes	1.30	0.44	0.67	2.62×10^{-2}	1.17×10^{9}	2.74×10^{9}	3.72×10^{-3}	0.28	9.38×10^{47}
39	Yes	0.42	0.23	0.16	2.43×10^{-2}	1.21×10^{8}	2.29×10^{9}	1.41×10^{-2}	0.75	2.04×10^{48}
43	Yes	0.41	0.22	0.16	2.26×10^{-2}	1.13×10^{8}	2.42×10^{9}	1.18×10^{-2}	0.49	2.17×10^{48}
47	No	0.45	0.24	0.15	2.54×10^{-3}	1.09×10^{8}	6.83×10^{8}	1.63×10^{-2}	0.57	1.24×10^{45}
48	Yes	0.54	—	0.21	4.81×10^{-2}	8.81×10^{7}	2.68×10^{9}	—	0.55	8.49×10^{48}
51	No	0.44	0.17	0.16	5.63×10^{-3}	1.12×10^{8}	3.96×10^{8}	1.09×10^{-2}	0.65	2.75×10^{43}
52	Yes	0.67	—	0.13	4.96×10^{-3}	8.48×10^{7}	2.29×10^{9}	—	0.64	8.12×10^{47}
57	Yes	0.85	0.29	0.32	3.13×10^{-2}	4.25×10^{8}	2.50×10^{9}	9.27×10^{-3}	0.38	6.09×10^{48}
58	Yes	1.20	0.27	0.32	7.80×10^{-2}	7.74×10^{8}	2.75×10^{9}	5.34×10^{-3}	0.41	2.03×10^{49}
61	Yes	0.85	0.28	0.32	2.52×10^{-2}	4.13×10^{8}	1.98×10^{9}	9.50×10^{-3}	0.33	4.70×10^{48}
62	Yes	1.21	0.15	0.30	9.15×10^{-2}	7.96×10^{8}	2.74×10^{9}	5.77×10^{-3}	0.45	2.53×10^{49}
66	Yes	1.20	0.15	0.35	5.15×10^{-2}	7.77×10^{8}	2.46×10^{9}	3.35×10^{-3}	0.74	1.86×10^{49}

4. SOME RESULTS
4.3 Characteristics of the interactions

Table 4. Hydrodynamical results for the simulations in which at least the material of one of the colliding stars does not remain bound to the remnant.

Run	Remnant	M_{WD} ($M_\odot$)	M_{debris} ($M_\odot$)	M_{ej} ($M_\odot$)	v_{ej} (km/s)	T_{max} (K)	T_{peak} (K)	E_{nuc} (erg)
3	No	—	—	1.80	—	—	1.70×10^{10}	1.42×10^{51}
4	Yes	1.20	0.37	0.43	6.06×10^{3}	7.89×10^{8}	9.00×10^{9}	1.35×10^{50}
7	No	—	—	1.80	—	—	1.70×10^{10}	1.72×10^{51}
8	Yes	1.20	0.39	0.41	5.95×10^{3}	7.66×10^{8}	8.51×10^{9}	1.42×10^{50}
37	Yes	0.37	0.06	0.16	3.19×10^{3}	9.16×10^{7}	2.75×10^{9}	1.61×10^{49}
38	No	—	—	0.80	—	—	4.02×10^{9}	7.45×10^{50}
40	No	—	—	0.80	—	—	4.03×10^{9}	7.24×10^{50}
41	Yes	0.78	0.02	0.41	1.22×10^{4}	2.76×10^{8}	3.57×10^{9}	3.67×10^{50}
42	Yes	1.20	0.01	0.39	1.30×10^{4}	7.08×10^{8}	3.97×10^{9}	3.76×10^{50}
44	No	—	—	0.80	—	—	4.06×10^{9}	7.38×10^{50}
45	Yes	0.77	0.02	0.41	1.22×10^{4}	3.05×10^{8}	3.66×10^{9}	3.66×10^{50}
46	Yes	1.20	0.01	0.39	1.32×10^{4}	7.14×10^{8}	4.18×10^{9}	3.93×10^{50}
49	Yes	0.79	0.01	0.40	1.21×10^{4}	2.63×10^{8}	3.57×10^{9}	3.46×10^{50}
50	Yes	1.20	0.01	0.39	1.29×10^{4}	6.89×10^{8}	3.58×10^{9}	3.67×10^{50}
53	Yes	0.80	0.01	0.40	1.15×10^{4}	2.03×10^{8}	3.54×10^{9}	3.16×10^{50}
54	Yes	1.20	0.01	0.40	1.27×10^{4}	6.99×10^{8}	3.62×10^{9}	3.58×10^{50}

4. WHITE DWARF COLLISIONS
Characteristics of the interactions

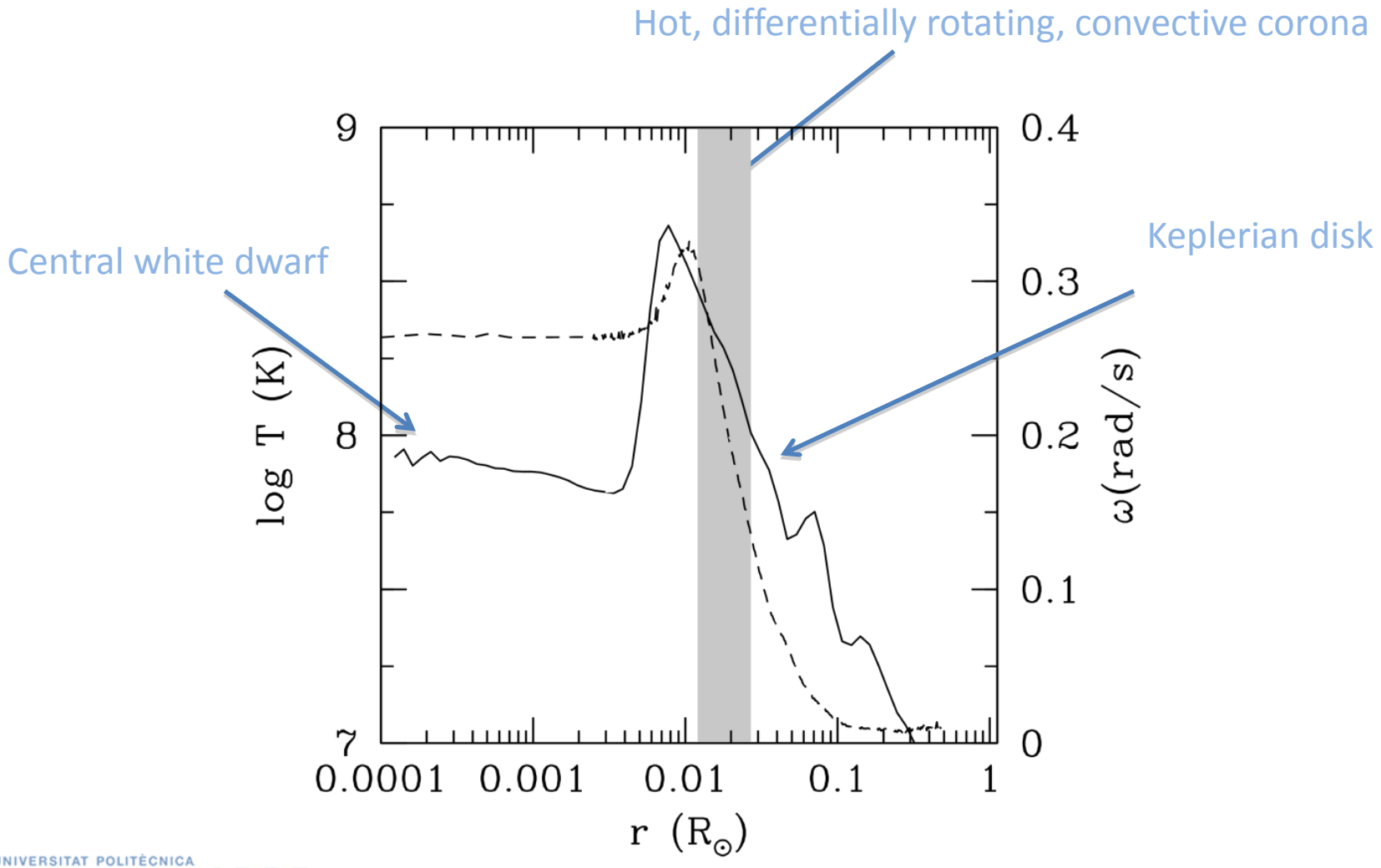

4. SOME RESULTS
4.3 Characteristics of the interactions

Table 5. Mass abundances of selected chemical elements (Mg, Si, and Fe), for the simulations in which a $0.8\,M_{\odot}$ and a $0.6\,M_{\odot}$ white dwarfs collide and form a bound remnant.

Run	1	5	9	13	17	21
β	2.83	2.81	1.57	1.22	0.68	0.66
$T_{\rm peak}$	4.37×10^{9}	4.50×10^{9}	3.03×10^{9}	2.18×10^{9}	1.16×10^{9}	9.22×10^{8}
Maximum abundances						
Mg	2.36×10^{-1}	2.33×10^{-1}	2.33×10^{-1}	2.12×10^{-1}	8.00×10^{-11}	1.95×10^{-14}
Si	5.86×10^{-1}	5.76×10^{-1}	2.39×10^{-1}	1.43×10^{-1}	1.31×10^{-16}	1.51×10^{-21}
Fe	3.54×10^{-3}	1.06×10^{-3}	5.03×10^{-24}	6.35×10^{-27}	5.20×10^{-34}	5.20×10^{-34}
Hot corona						
⟨Mg⟩	1.98×10^{-7}	4.14×10^{-7}	9.87×10^{-8}	1.53×10^{-12}	1.50×10^{-22}	3.12×10^{-24}
⟨Si⟩	1.50×10^{-9}	6.04×10^{-9}	5.51×10^{-10}	6.64×10^{-17}	3.38×10^{-31}	1.03×10^{-33}
⟨Fe⟩	5.20×10^{-34}	5.20×10^{-34}	5.19×10^{-34}	5.20×10^{-34}	5.15×10^{-34}	5.09×10^{-34}
Debris region						
⟨Mg⟩	2.97×10^{-3}	2.74×10^{-3}	1.16×10^{-3}	2.48×10^{-5}	1.04×10^{-14}	2.28×10^{-18}
⟨Si⟩	7.17×10^{-3}	5.71×10^{-3}	5.84×10^{-4}	1.16×10^{-5}	1.57×10^{-20}	1.30×10^{-25}
⟨Fe⟩	5.14×10^{-7}	2.60×10^{-7}	4.49×10^{-28}	3.81×10^{-31}	4.63×10^{-34}	4.42×10^{-34}
Ejecta						
⟨Mg⟩	5.92×10^{-2}	5.81×10^{-2}	1.58×10^{-2}	5.72×10^{-10}	6.38×10^{-18}	3.24×10^{-17}
⟨Si⟩	1.27×10^{-1}	1.29×10^{-1}	9.27×10^{-3}	3.84×10^{-14}	3.07×10^{-25}	2.73×10^{-24}
⟨Fe⟩	2.16×10^{-6}	3.15×10^{-6}	2.97×10^{-27}	4.10×10^{-34}	5.20×10^{-34}	5.20×10^{-34}

4. SOME RESULTS
4.3 Characteristics of the interactions

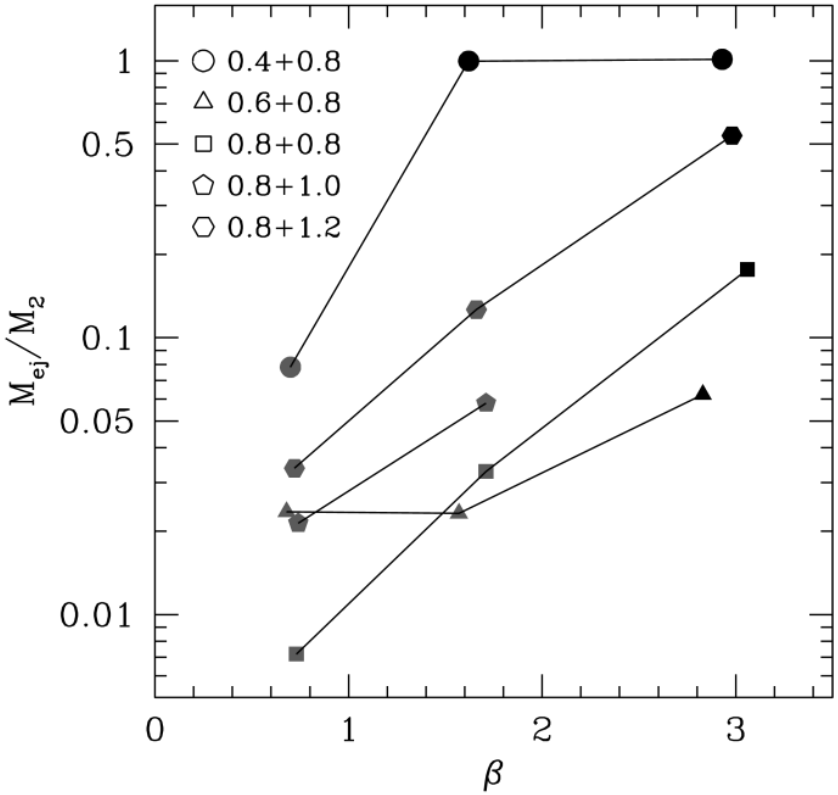

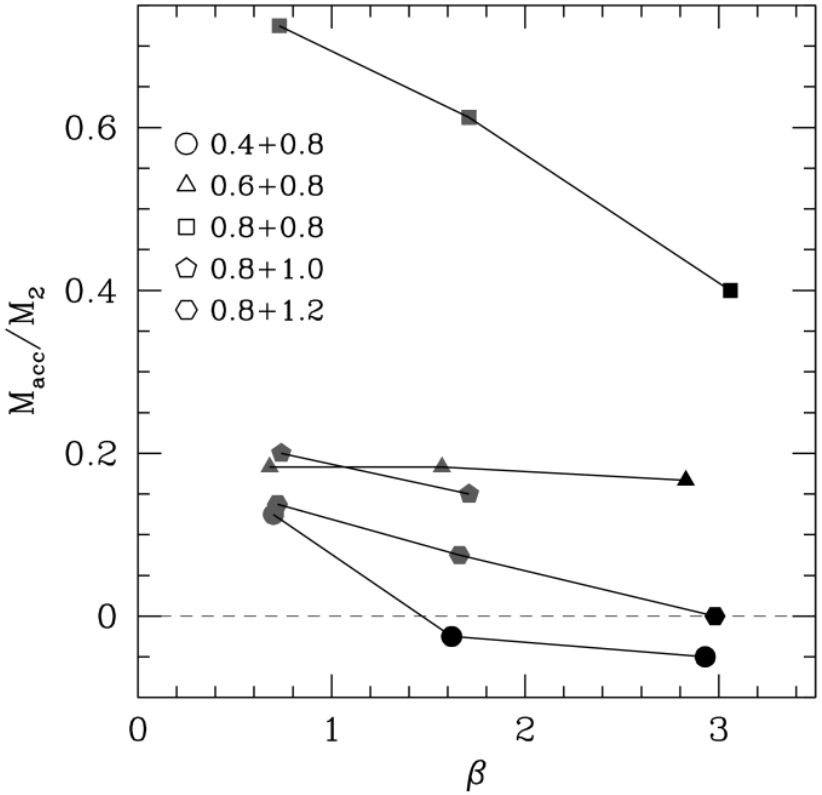

4. SOME RESULTS
4.3 Characteristics of the interactions

Run	Detonation	Ni ($M_\odot$)
37	L	1.31×10^{-9}
38	B	8.84×10^{-4}
39	Y	5.57×10^{-16}
40	B	1.64×10^{-3}
41	L	8.04×10^{-4}
42	L	1.18×10^{-3}
43	Y	4.97×10^{-14}
44	B	4.68×10^{-3}
45	L	7.60×10^{-4}
46	L	2.21×10^{-3}
48	Y	2.76×10^{-11}
49	L	5.00×10^{-4}
50	L	9.36×10^{-4}
52	Y	1.62×10^{-17}
53	L	2.00×10^{-4}
54	L	8.44×10^{-4}
57	Y	6.98×10^{-14}
58	Y	5.61×10^{-10}
61	Y	2.37×10^{-16}
62	Y	3.27×10^{-9}
66	Y	7.30×10^{-12}

Run	Detonation	Ni ($M_\odot$)
1	Y	8.65×10^{-8}
2	Y	4.47×10^{-3}
3	B	7.25×10^{-1}
4	L	6.60×10^{-2}
5	Y	2.74×10^{-8}
6	Y	3.67×10^{-3}
7	B	7.15×10^{-1}
8	L	6.32×10^{-2}
9	Y	7.89×10^{-34}
10	Y	4.52×10^{-10}
11	Y	7.94×10^{-7}
12	Y	1.09×10^{-5}
14	Y	7.44×10^{-16}
15	Y	1.56×10^{-13}
16	Y	9.70×10^{-10}
20	Y	1.12×10^{-33}
24	Y	1.12×10^{-33}

4. SOME RESULTS
4.3 Characteristics of the interactions

- The peak temperatures reached in the interactions are typically 10^9 K, driving extensive nucleosynthesis in the shocked regions.
- Two interactions result in a powerful detonation, producing a SNIa outburst.
- Some other simulations result in bound remnants with masses close to the Chandrasekhar limit.
- A wide range of masses of ^{56}Ni is produced, which may explain some underluminous transients.

4. SOME RESULTS
4.4 Observational signatures

- Gravitational wave emission in the slow-motion, weak-field, quadrupole approximation (Misner et al. 1973).
- Late-time bolometric light curve, using a Monte Carlo code which solves the transport of photons, and the injection of energy by γ-rays produced by the ^{56}Ni and ^{56}Co decays (Kushnir et al. 2013).
- Thermal neutrino emission, using the rates of Itoh et al. (1997).
- Fallback accretion X-ray luminosity (Rosswog 2007).

4. SOME RESULTS
4.4.1 Gravitational waves

Eccentric orbits

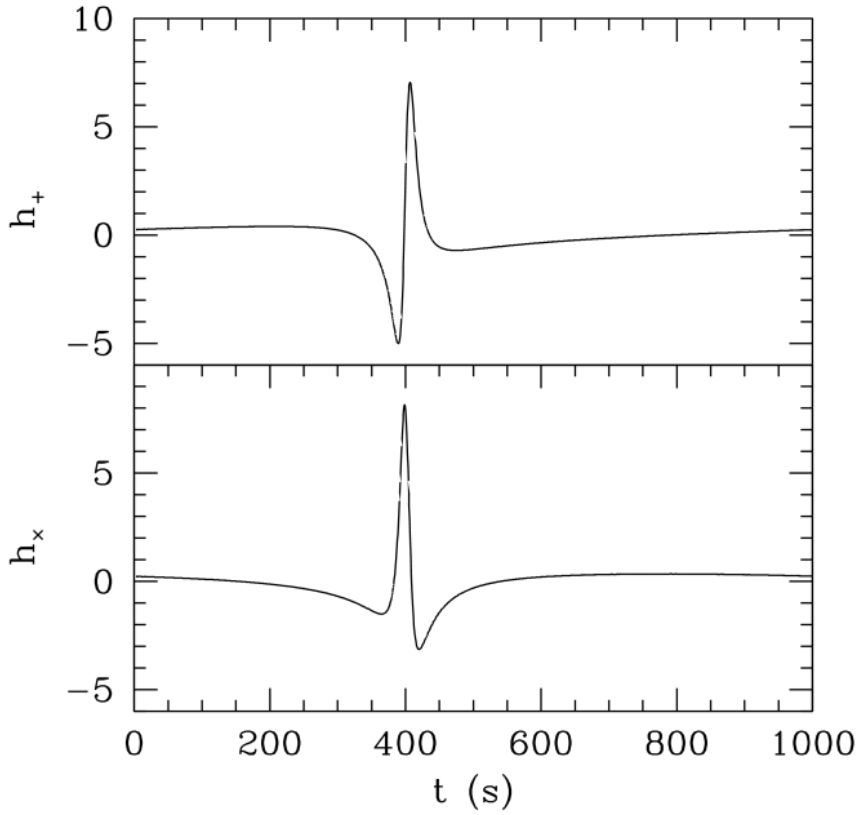

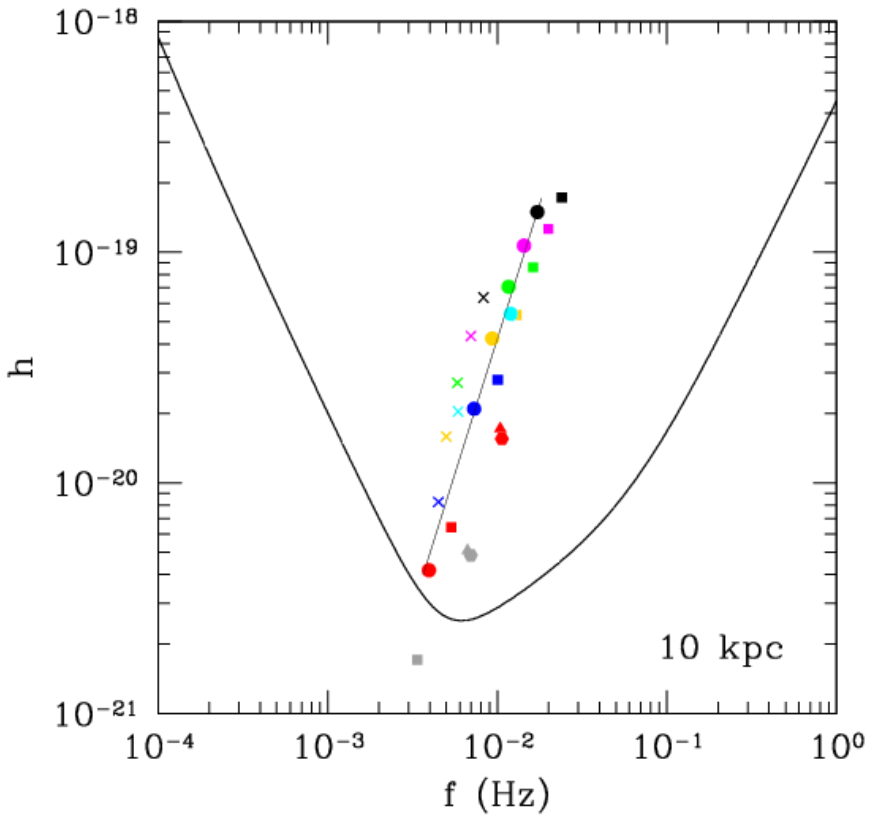

$0.8\ M_\odot + 0.8\ M_\odot$ $0.8\ M_\odot + 1.2\ M_\odot$ $0.4\ M_\odot + 1.2\ M_\odot$ $0.4\ M_\odot + 0.4\ M_\odot$

$0.8\ M_\odot + 0.6\ M_\odot$ $0.8\ M_\odot + 1.0\ M_\odot$ $0.8\ M_\odot + 0.4\ M_\odot$ $0.4\ M_\odot + 0.2\ M_\odot$

4. SOME RESULTS
4.4.1 Gravitational waves

Lateral collisions

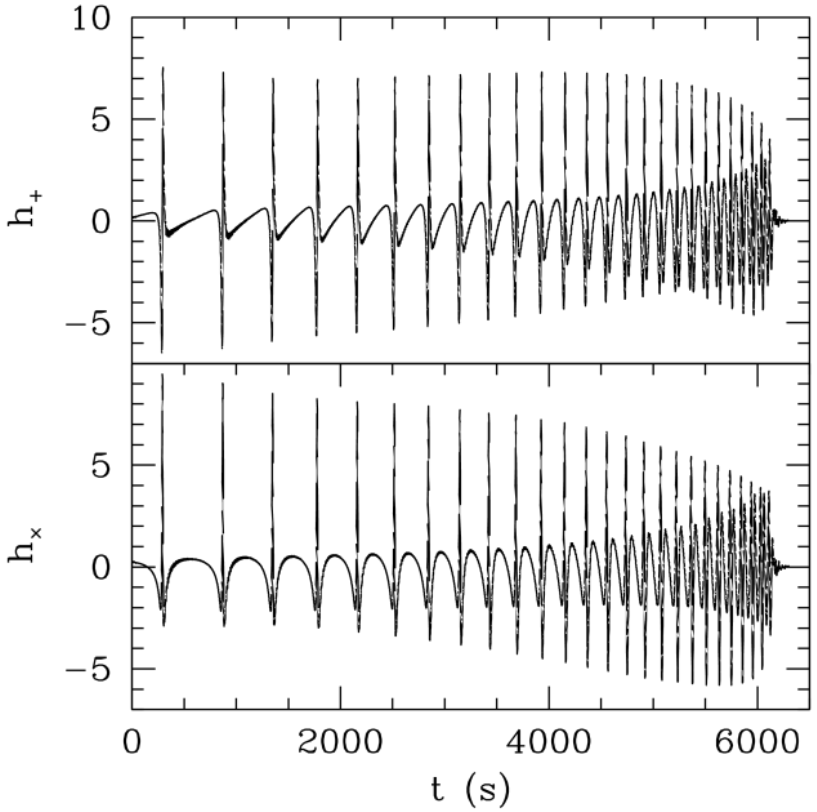

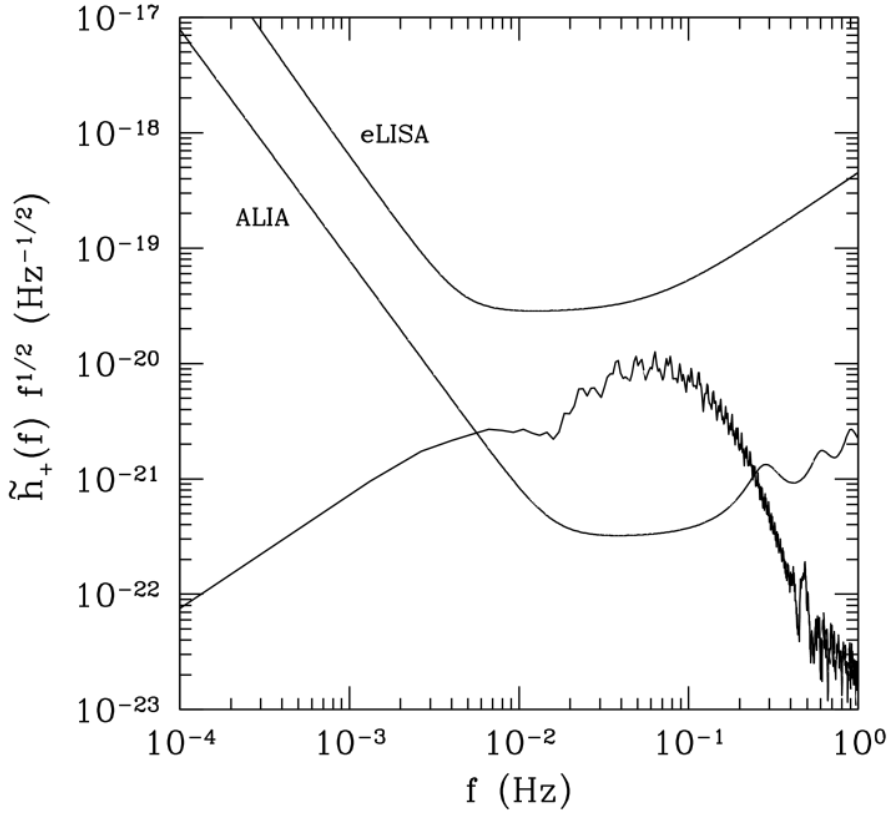

4. SOME RESULTS
4.4.1 Gravitational waves

Direct collisions

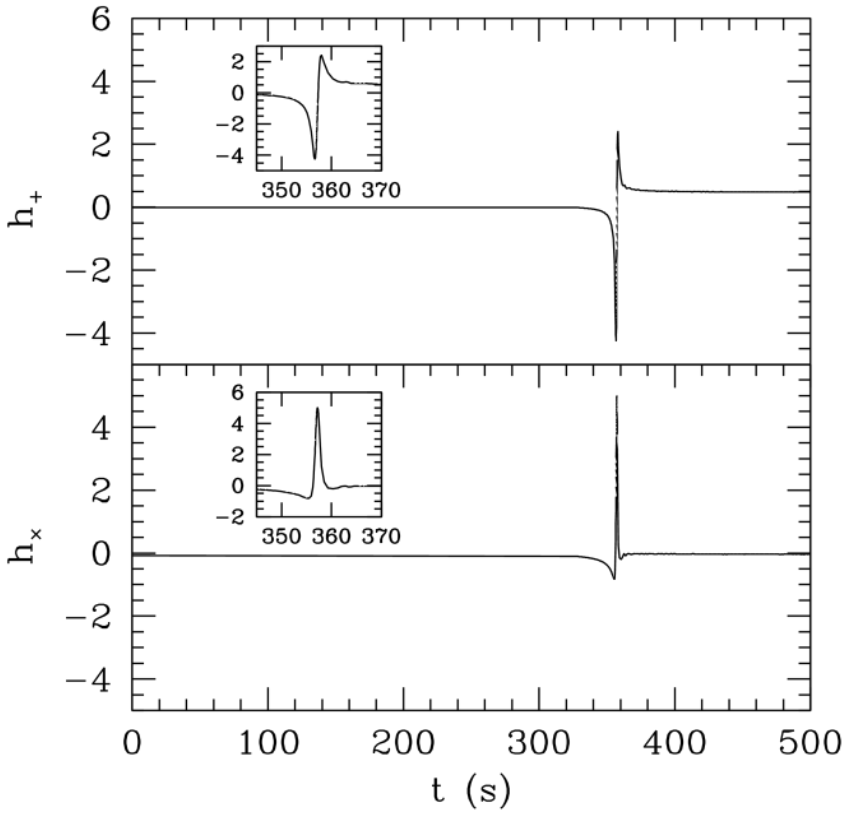

4. SOME RESULTS
4.4.2 Light curves

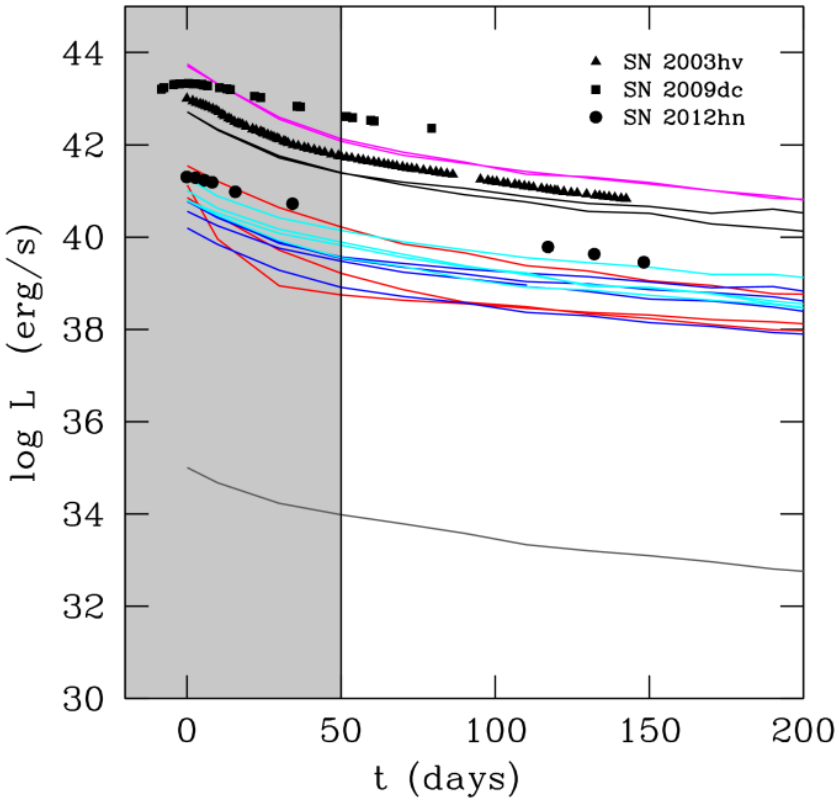

$0.8\ M_\odot + 1.2\ M_\odot$ $0.4\ M_\odot + 1.2\ M_\odot$ $0.4\ M_\odot + 0.4\ M_\odot$

$0.8\ M_\odot + 1.0\ M_\odot$ $0.8\ M_\odot + 0.4\ M_\odot$ $0.4\ M_\odot + 0.2\ M_\odot$

4. SOME RESULTS
4.4.3 Thermal neutrinos

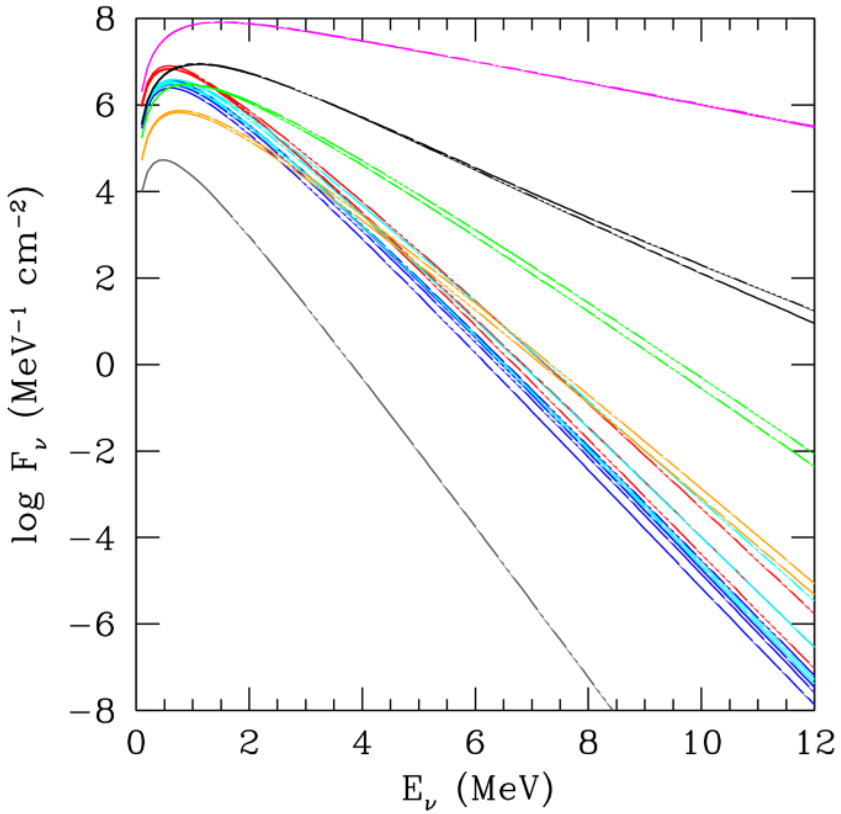

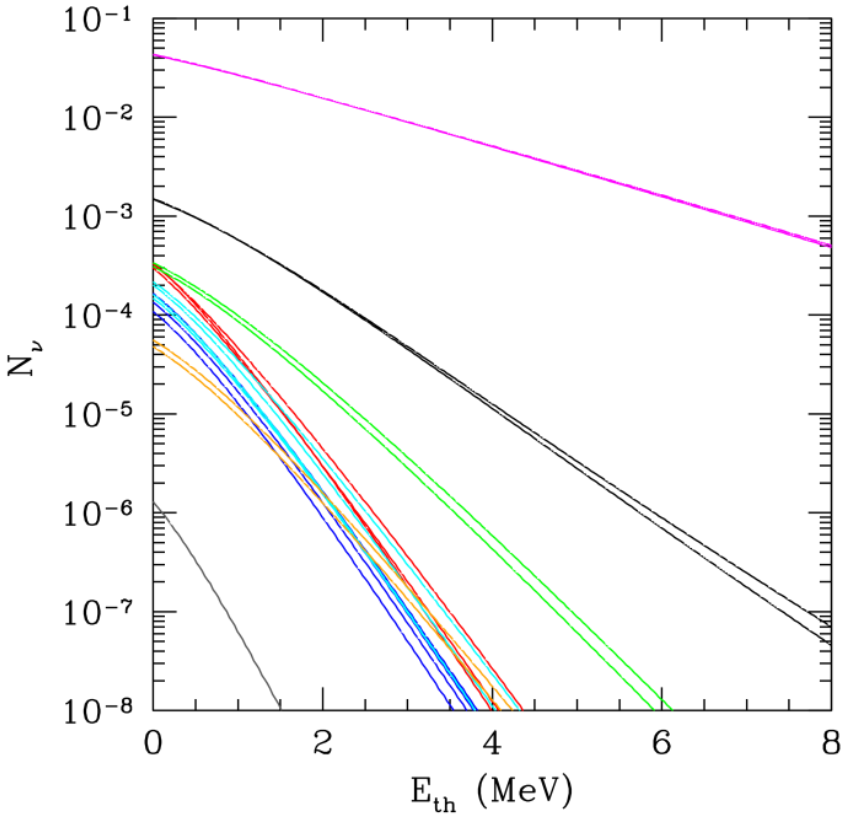

$0.8\ M_\odot + 0.8\ M_\odot$ $0.8\ M_\odot + 1.2\ M_\odot$ $0.4\ M_\odot + 1.2\ M_\odot$ $0.4\ M_\odot + 0.4\ M_\odot$

$0.8\ M_\odot + 0.6\ M_\odot$ $0.8\ M_\odot + 1.0\ M_\odot$ $0.8\ M_\odot + 0.4\ M_\odot$ $0.4\ M_\odot + 0.2\ M_\odot$

4. SOME RESULTS
4.4.4 Fallback luminosities

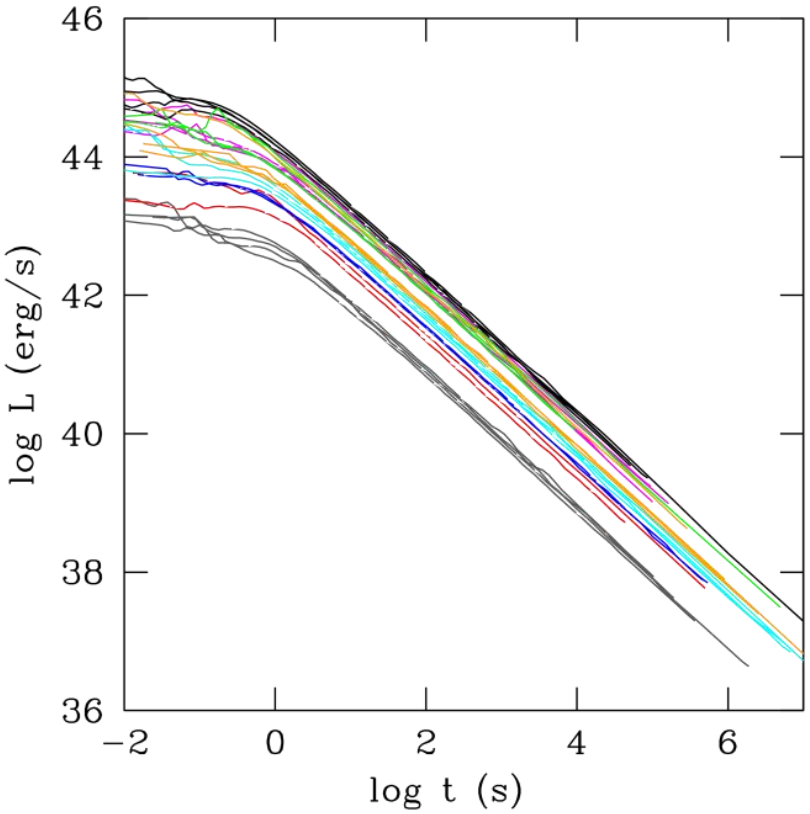

$0.8\ M_\odot + 0.8\ M_\odot$ $0.8\ M_\odot + 1.2\ M_\odot$ $0.4\ M_\odot + 1.2\ M_\odot$ $0.4\ M_\odot + 0.4\ M_\odot$

$0.8\ M_\odot + 0.6\ M_\odot$ $0.8\ M_\odot + 1.0\ M_\odot$ $0.8\ M_\odot + 0.4\ M_\odot$ $0.4\ M_\odot + 0.2\ M_\odot$

4. SOME RESULTS
4.4 Observational signatures

- A combination of optical and high-energy observations, and data from the future space borne gravitational wave detectors would provide in valuable insight on the conditions under which these interactions occur.
- Only those interactions involving two rather massive white dwarfs (masses larger than 0.8 $M_{\odot}$) would have light curves resembling those of type Ia SNe.

CONTENTS

5. Conclusions

- I have reviewed the results of the most comprehensive suite of simulations of white dwarf collisions available so far:
  - Three possible outcomes are obtained: eccentric orbits, and lateral or a direct collisions.
  - We have determined the areas in the parameter space where they are found.
  - In several direct collisions the material of the secondary star is ignited explosively, being this more frequent for He WDs.
  - In the most violent collisions both stars are totally disrupted and no bound remnant is obtained, whereas in other cases only the secondary is disrupted.

5. Conclusions

- The gravitational waves radiated in those interactions in which the outcome is an eccentric binary could be eventually detected by eLISA.
- There are little hopes to detect the emission of thermal neutrinos.
- The late-time bolometric light curves show large variations. Those corresponding to the most violent collisions are very similar to those of SNe Ia, while those of less violent interactions could explain underluminous transients.
- The fallback luminosities follow a power law with index -5/3, and could be easily observed.

UNIVERSITAT POLITÈCNICA DE CATALUNYA BARCELONATECH

IEEC

White dwarf collisions: a new pathway to type Ia supernovae

Enrique García-Berro & Pablo Lorén-Aguilar

Supernovae, hypernovae and binary driven hypernovae

An Adriatic Workshop – Pescara 2016